



NUMERICAL SIMULATION OF FALLING FILM THICKNESS FLOWING OVER HORIZONTAL TUBES

Ibnu Anas Hassan, Azmahani Sadikin and Norasikin Mat Isa

Department of Plant and Automotive Engineering, Universiti Tun Hussein Onn Malaysia, Parit Raja, Batu Pahat, Johor, Malaysia

E-Mail: hd130018@siswa.uthm.edu.my

ABSTRACT

This paper presents a numerical simulation of water falling film flowing over horizontal tubes. The objective of this study is to use numerical predictions for comparing the thickness of falling liquids film on CFD models with a verification of previous literatures. A comprehensive design of 3-D models have been developed and validated by the real application of the falling film evaporator as well as experimental parameters often used in the past literatures. A computational fluid dynamic simulation of the water falling film is presented using the Volume of Fluid (VOF) technique. The Volume of Fluid (VOF) technique is capable of determining the thickness of falling liquids film on tubes surface under the influence of the pitch tube and at low pressures. Four types of CFD numerical models with different pitch tubes of 70.05 mm, 59.05 mm, 47.35 mm and 26.85 mm were used in this simulation. The use of a numerical simulation tool on water falling film has resulted in a detailed investigation of film thickness. Based on the numerical simulated results, it is found that the average values of water film thickness for each model are 0.1858 mm, 0.1904 mm, 0.2052 mm, and 0.2200 mm.

Keywords: CFD, horizontal tubes, falling film, falling film thickness, VOF.

INTRODUCTION

A falling liquids film flow over a surface of a horizontal tube has been widely used as a configuration of heat exchanger. This type of heat exchanger has made a number of important technical applications ranging from desalination devices, refrigeration, chemical, food and dairy industries. The configuration of horizontal tube falling film evaporator is the design standard for sea water desalination devices which mostly for multiple effect distiller including Mechanical Vapour Compression (MED-MVC) Evaporator systems.

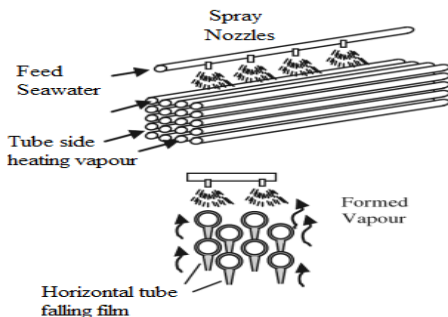


Figure-1. Configuration of horizontal tube falling film evaporator. (H. Ettouney).

It has been extensively utilized in this system because of many advantages such as high heat transfer rates at low liquid flow rates, small temperature differences and pressure drop over the tubes is negligible. The increasing use of falling film technology in seawater desalination application has brought an impact to the conventional heat exchangers such as the coil and flooded evaporators. They have received less attention and being replaced gradually in recent years.

The flow mode classification of a falling liquid film that occur in such configurations plays an important role in the heat and mass transfer process of falling film evaporator. The complex nature of these events has received wide attention from many researchers. Many theoretical and experimental studies has provided valuable contributions. They are generally observed by means of control over the mass flow rate of the falling liquid film and other physical parameters such as pitch length, shape of tube surface, and kinds of fluids used [1]. Basically, there are three different patterns of flow modes can be observed when falling liquid films flow over horizontal cylinders. These are droplet mode, the jet or column mode and the sheet mode as shown in Figure-2.

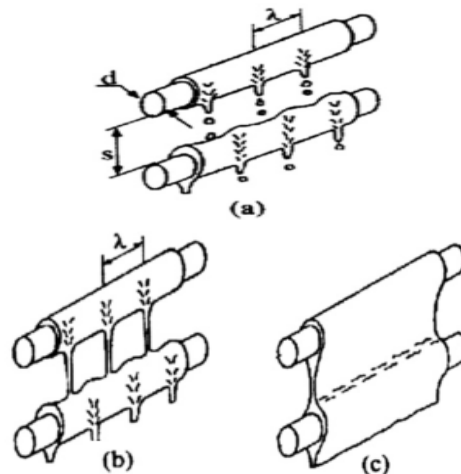


Figure-2. Schematic of the three main flow modes a) droplet mode, b) column or jet mode and c) sheet mode. [2]



Apart from that, there are two other patterns of transition regions exists between these three main stable flow modes described previously. Each mode is known as droplet-columnar and columnar-sheet

LITERATURE REVIEW

A better understanding of the falling film flow patterns, heat and mass transfer is not impossible to achieve. Moreover, Computational Fluid Dynamics (CFD) has been developed in the last decade. Recently, various numerical simulation methods have been developed to model this flow mode. Many researchers such as [3], [4], [5] have developed a numerical simulation framework for detailed investigation of falling liquid film on horizontal tubes.

Based on the experimental work and the numerical simulation on horizontal tube bundle, [3] reveals that the flow pattern varies with different flow rates. The arrangement of tubes is staggered and three tubes form a triangular configuration of three-dimensional CFD model.

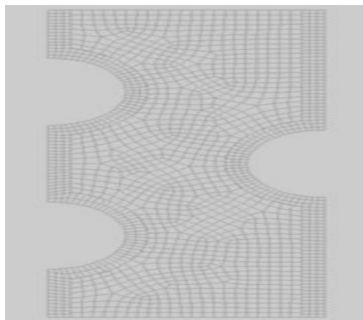


Figure-3. Schematic of a triangular configuration of three-dimensional CFD model. [3]

The numerical simulated results are compared with experimental results under similar conditions to validate its accuracy.

Table-1. Simulation result comparison with experiment result. [3]

Flow pattern	Simulation results (kg/s)	Experiment results (kg/s)
Droplet	$Q < 2 \times 10^{-3}$	$Q < 2.1 \times 10^{-3}$
Droplet-column	$2 \times 10^{-3} < Q < 1.25 \times 10^{-2}$	$2.1 \times 10^{-3} < Q < 1.3 \times 10^{-2}$
Column	$1.25 \times 10^{-2} < Q < 1.75 \times 10^{-2}$	$1.3 \times 10^{-2} < Q < 1.7 \times 10^{-2}$
Column-sheet	$1.75 \times 10^{-2} < Q < 2 \times 10^{-2}$	$1.7 \times 10^{-2} < Q < 2.15 \times 10^{-2}$
Sheet	$Q > 2 \times 10^{-2}$	$Q > 2.15 \times 10^{-2}$

The significant effects of heat transfer on falling film thickness is discussed many years. Results of experiments by D. Gstohl, J.R. Thome has been reviewed by [6] suggests that the increase in the film thickness sheet mode can reduce the heat transfer coefficient. Film thickness increases with the flow rate of the water film. Other facts that support the effect of increasing the heat transfer to a thinner film thickness can be obtained on a review by [7]

[5] investigated numerically the influence of hydrodynamics, mass flow rate, the feeder height on the distribution of the film thickness and heat transfer characteristics of the liquid falling film on non-circular enhanced tubes. The study was conducted by using 3 types of two-dimensional CFD model with different shapes. Each model is designed with a single horizontal tube and symmetrical halves.

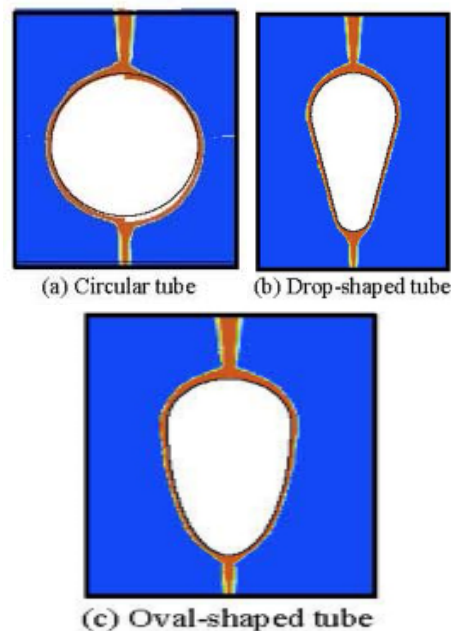


Figure-4. Three types of two-dimensional CFD model with different shapes. [5]

The models examined are considered for use in sea water desalination. The numerical simulation results show that the minimum value of the film thickness appears approximately at the angular positions of 125°, 60° and 170° for the smooth circular, oval- and drop-shaped tubes, respectively. The film thickness grows with the increase of the mass flow rate and decrease of the feeder height. The variation of flow pattern varies for different tubes.

Recently, [8] has simulated an experiment with a two-dimensional CFD model. It was designed by adapting three horizontal cylinders. The arrangement of these cylinders on CFD model are in a single column, but it was under condition of the half-symmetry of domain. This symmetrical condition aimed to obtain a faster solution.

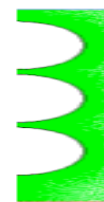


Figure-5. CFD numerical model with three cylinders on half-symmetry of numerical domain.



The numerical results have been compared with the present experimental results as well as those from the literature. The flow modes and film thickness are reported for the Reynolds numbers range of 400 and 3200. Sets of experiments are conducted using water as the test fluid, and at mass flow rates of 0.1 and 0.2 kg/ms. It is found that the falling-liquid film modes are the jet-sheet and sheet modes, respectively. He also simulated 2D numerical model of water falling film and compared its thickness with previous literature as shown in Figure-6 below.

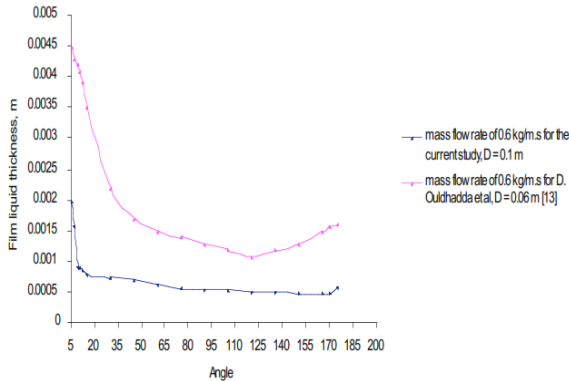


Figure-6. The graph of film thickness of water falling on a circular horizontal tube. [8].

Water film thickness has been calculated according to equation of Rogers and Goindi [8]. This equation can only give a film thickness at orientation angle of 90 degrees as shown in Figure-12.

$$\left(\frac{\delta}{d}\right)_{\min} = 1.186 Re^{\frac{1}{2}} Ar^{-\frac{1}{2}} \quad (1)$$

Ar = Archimedes Number, 10^{10}

In addition, the review of [9] shows that experimental results of [10] have proposed a new correlation for measuring the film thickness. The correlation has an advantage compared with equation 1. It can provide the expected value of the plain tube film thickness in the range 0-180°

$$\delta = c \left(\frac{3 \mu_L \Gamma}{\rho_L (\rho_L - \rho_g) g \sin \beta} \right)^{\frac{1}{3}} \left(\frac{S}{D} \right)^n \quad (2)$$

Modeling the flow behavior of falling liquid film on horizontal tube needs more details and extensive investigations. The most simple configuration of CFD numerical model has only one tube to speed analysis process [5]. Many previous literatures such as [3], [8] and [11] have been designed with more than one tube including staggered or in-line arrangement.

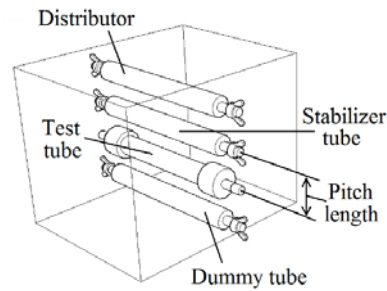


Figure-7. The simplest configuration of falling liquid film test rig by [2].

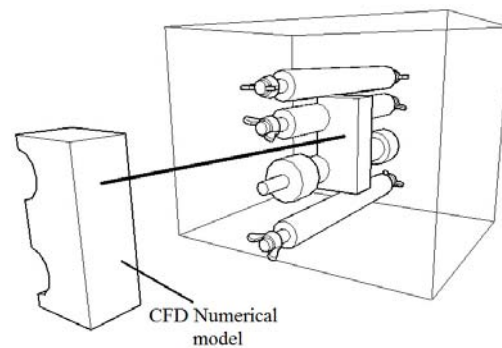


Figure-8. The CFD numerical model in test section. [2].

Although many numerical studies have been carried out on falling film thickness, there is still no work involving measurement of falling film thickness flowing over horizontal tube on 3D CFD model. The present work performs numerical predictions of falling film thickness compared with those obtained with different pitch tubes including theoretical value.

METHODS AND MATERIALS

Physical model

The physical geometry of numerical model is constructed using Fluent simulation software with a local body of influence techniques in meshes. The single in-line arrangement of two tubes formed a configuration as shown in Figure-9.

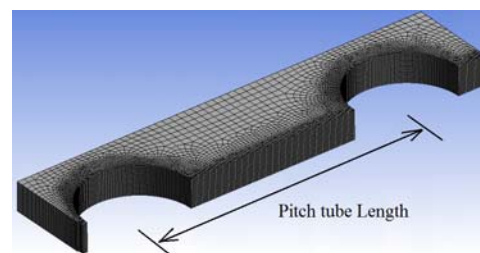


Figure-9. The pitch tubes length between two tube axes.

Both tubes have diameter of 19.05mm with 4 different pitch tubes. These are 70.05 mm, 59.05 mm,



47.35 mm and 26.85 mm. The tube cylinder wall are considered as a smooth surfaces with temperature of 60°. The width of these numerical models is 5 mm to reduce number of elements for a better and small mesh refinement size.

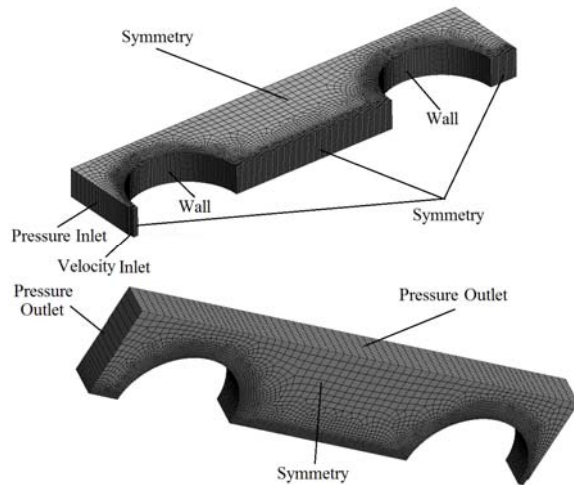


Figure-10. Boundary conditions for 3dimensional CFD numerical model.

The boundary for water flow inlet is on top surface of the CFD numerical model. It was set as a velocity inlet, where the water liquid flows downward uniformly at different velocities. The remaining top and back boundaries are set as the pressure inlet while the bottom boundary is the pressure outlet. The front and both sides of this model are considered as the symmetrical boundary conditions.

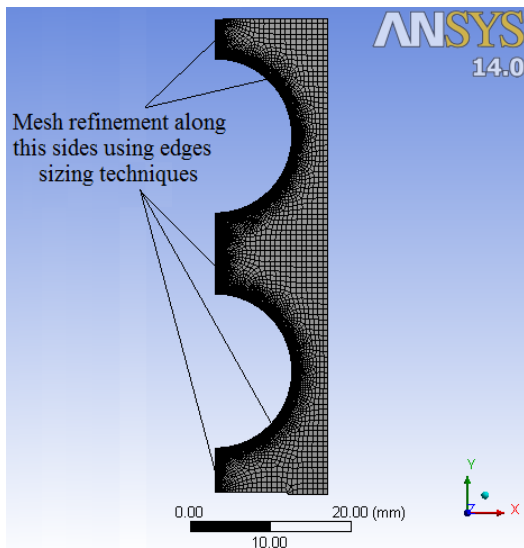


Figure-11. The surfaces along left edges of CFD model is carefully meshed.

The adjacent region around the tube wall and along symmetry line are carefully refined using a face sizing techniques. All mesh refinement size is 0.2 mm and applied with fluent default setting. This refinement technique making it possible to observe the thickness of falling liquid film in detail near the test tube surface. The falling water film flows over the upper tube is under combined effect of the gravity to the bottom of test tube. The flow is also directly influenced by adhesive and viscosity characteristics of water to the walls of the tubes.

Properties of fluids

In this simulation analysis, water is used as the working fluids. The flow behaviour of working fluids mostly depend on Reynolds Number of liquid film and it is defined according to

$$Re_L = \frac{\rho \Gamma}{\mu} \quad (3)$$

Re_L = film Reynolds number

Γ = film flow rate per unit of tube length

μ = Newtonian dynamic viscosity of liquid film

A high mass flow rate of falling films is normally producing turbulent flow when Reynolds number is larger than 1600, while Re lower than 1600 usually gives laminar flow. The flow range of falling films applied in this simulation was treated as being laminar since its $Re = 800$. The turbelant flow settings will take over the sheet flow mode. All properties of fluids are listed, as shown in Table-2.

Table-2. Properties of test fluids.

Properties	Values
Water density (kg/m^3)	996.6
Water viscocity (kg/ms)	8.538e-4
Air density (kg/m^3)	1.176
Air viscocity (kg/m-s)	1.8582e-5
Temperature	27°C
Pressure	101.42kPa

Numerical Methodologies

The Volume of Fluid (VOF) model was selected for simulation with assumption that some of water evaporation is neglected. It is useful tool for tracking free surface flow on tubes. The volume fraction figures shows the film distribution on the wall of tubes and flow patterns between tube spacing. These characteristics will vary with flow rate. The explicit scheme allows analysis to use variable time stepping in order to automatically change the time-step when an interface is moving through dense cells or if the interface velocity is high.



In Ansys Fluent, the boundary conditions of water inlet only deal with flow velocity. It has been determined using velocity inlet of liquid film, V_L

$$V_L = \frac{Re_f \mu}{\rho l} \quad (4)$$

Re_f = film Reynolds number
 l = Length of tube, 0.25 m
 μ = Newtonian dynamic viscosity of liquid film
 ρ = Mass density
 A = Surface area of water inlet, $0.734424 \times 10^{-2} \text{ m}^2$ for 86 holes with 1mm in diameter in real test facility design.

The evaluation of the flow modes transformation were simulated at temperature and pressures of 27°C and 101.42kPa respectively. The velocity inlet of water corresponding to Reynold Number 800 is 0.6469m/s. The laminar flow start at velocity inlet V_L 1.27 m/s. Table-3 summarizes all simulation settings of Ansys Fluent software for this CFD model.

Table-3. Fluent simulation settings.

Setting	Option
Solver	Transient
Model	VOF
Fluids	Water liquid and air
Viscous model	Laminar for V_L 1.27 m/s
Pressure-velocity coupling	PISO for incompressible
Pressure	Body force weighted
Momentum	2nd order upwind
Energy	1st order upwind
Volume fraction	Geo-reconstruct
Surface tension force	CSF model (continuum surface force)
Time steps	Variable

The velocity inlet is close to experimental range used by [2] which is 2.3 kg/ms. It was iterated using Ansys Fluent software until sheet flow mode condition is existed on four CFD models. Initially, this parameter is predicted carefully based on previous literatures using equations 3 and 4. Four different types of CFD models with pitch tubes of 70.05 mm, 59.05 mm, 47.35 mm and 26.85 mm are provided for this analysis. The corresponding mass flow rate to its velocity inlet is then recorded when a proper film distribution is achieved in simulation result. The data of simulation are extracted separately into several folders in order to avoid huge file generated by Ansys Fluent. The bigger size of file is easily tend to become a corrupted files.

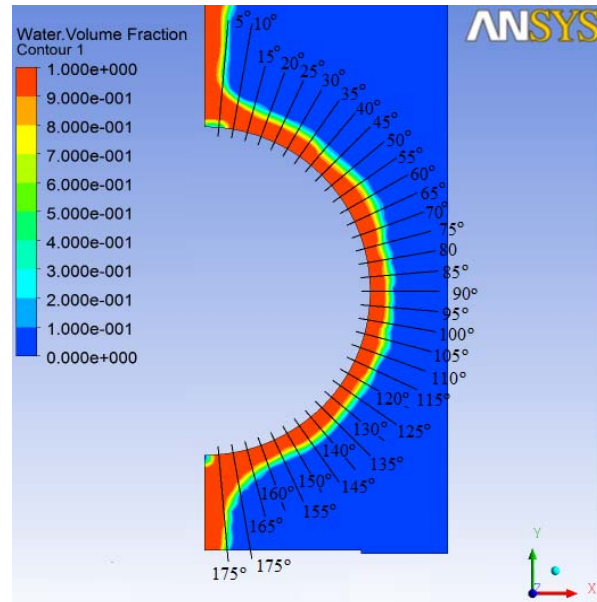


Figure-12. The orientation angles of film thickness measurements on tube surface.

The thickness of water sheet film on tube surface is then measured based on angles of 15°, 30°, 45°, 60°, 75°, 90°, 105°, 120°, 135°, 150° and 165° as shown in Figure-12. These angles have been set as a reference values in accordance with many previous references such as [8]. The numerical results are analyzed in CFD-Post where 4.5mm and 6.75mm in length of measurement lines were adapted normal to tube surface. These measurement lines acted as a parameters that measures water film thickness at local point and specified angles on tube surface as shown in Figure-11. There are 6 measurement lines were adapted in a singlerow namely 1, 2, 3, 4, 5 and 6 as shown in Figure-13. Each row of measurement lines is in parallel with the tube axis. The corresponding values of film thickness on the same plane are based on their orientation angles respectively. The volume of fraction that is acceptable is 1 which indicated 100% water.

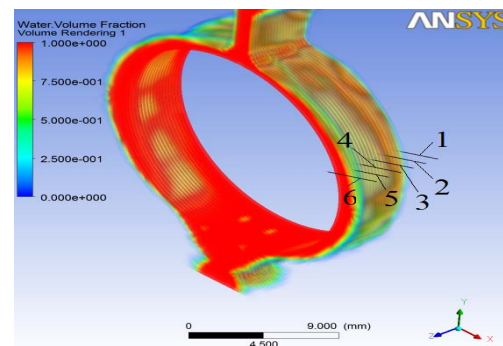


Figure-13. The positions of measurement lines in a single row of 70° orientation angle.

The thicknesses of water film are plotted in a graph of thickness versus orientation angles. Each



measurement line is measured by taking into account the difference of water volume fraction length of 1. The average values of a row represent the whole thickness of water film at the corresponding angle.

SIMULATION RESULTS AND DISCUSSIONS

A series of simulation process were carried out to observe the effect of water film thickness on water falling film under the influence of tube spacing and low pressures. In the following, we first present typical simulation results of water film thickness for sheet flow modes. These visual result are shown in Figure-13-16. The results of numerical analysis is ended when each flow on model has been completely transformed into sheet flow mode. In addition, all results must converged before analysis ended.

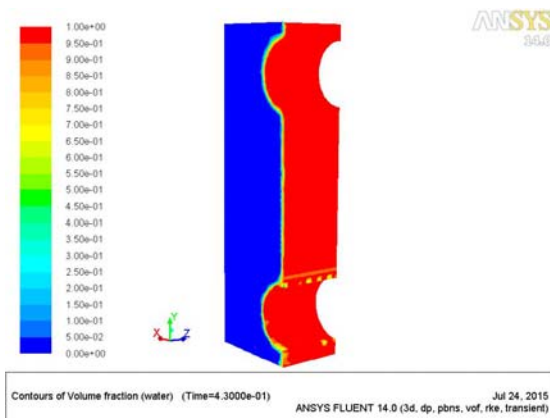


Figure-14. Sheet flow mode for 3-dimensional model with pitch tube of 70.05 mm and water mass flow rates 0.17kg/ms.

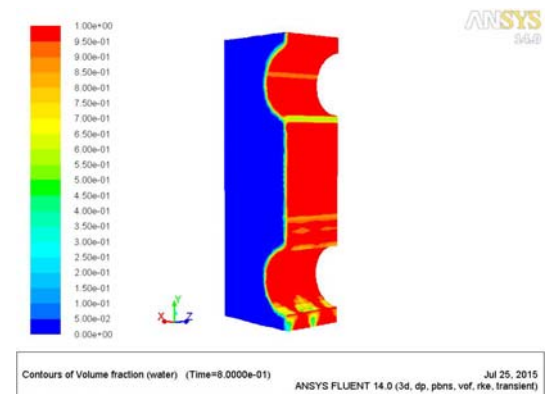


Figure-15. Sheet flow mode for 3-dimensional model with pitch tube of 59.05 mm and water mass per unit tube 0.17 kg/ms.

There are a few spots and lines of yellow contour on Figure-13-16. This contour indicates a condition of water vapor and it is represented by water volume fraction between 60-70%. In addition, this condition existed at the bottom of the tube due to separated flow.

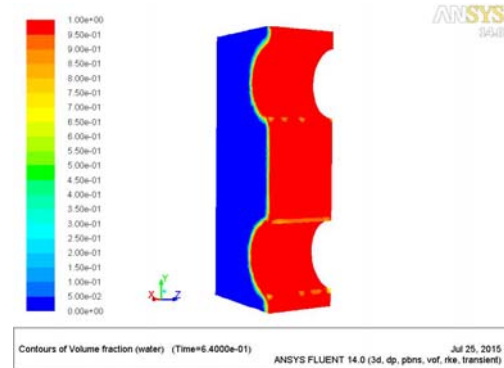


Figure-16. Sheet flow mode for 3-dimensional model with pitch tube of 47.35 mm and water mass flow rates per unit tube 0.17kg/ms.

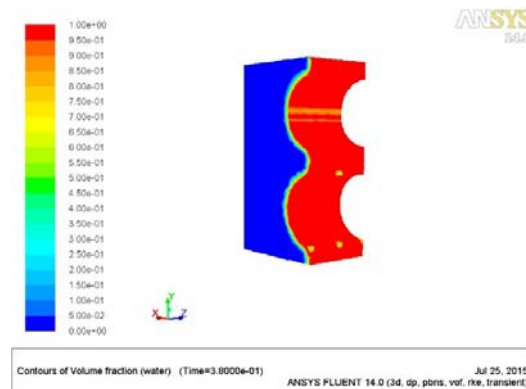


Figure-17. Sheet flow mode for 3-dimensional model with pitch tube of 26.85 mm and water mass flow rates per unit tube 0.17 kg/ms.

Table-4. The film thickness of four different pitch tubes.

Orientation of angles	The thickness of falling liquids film on different pitch tubes (mm)			
	70.05	59.05	47.35	26.85
15	0.1641	0.1102	0.5531	0.3351
30	0.1132	0.0325	0.0348	0.0605
45	0.1648	0.1491	0.2018	0.1872
60	0.1614	0.2152	0.0493	0.2231
75	0.1354	0.2904	0.1144	0.1401
90	0.1065	0.1020	0.0863	0.0785
105	0.0546	0.1777	0.2881	0.1513
120	0.1959	0.1969	0.0762	0.1760
135	0.2572	0.1505	0.1401	0.1031
150	0.2597	0.1695	0.1155	0.3559
165	0.4308	0.5000	0.5977	0.6091
Average	0.1858	0.1904	0.2052	0.2200



The average thickness of sheet flow mode on four CFD numerical models have been compared in Table-4. The setting for sheet flow is laminar mode as its inlet velocity not exceeds 0.2 m/s. This value can be determined by equation 3.

Based on a comparative Table-4, the average thickness of the highest pitch tube produced the thinner film. The average thickness of simulation results for all four CFD numerical models are 0.1858mm, 0.1904 mm, 0.2052 mm and 0.2200 mm. When this data is plotted on graph in Figure-17, four different paths of CFD models are presented. The thickness is varies according to the angular positions and pitch tubes. It becomes relatively low in range between 30° to 150° as shown in Figure-18. In theory, the film thickness at any orientation angle can be calculated by equation 2 and equation 1 is only applied to 90°.

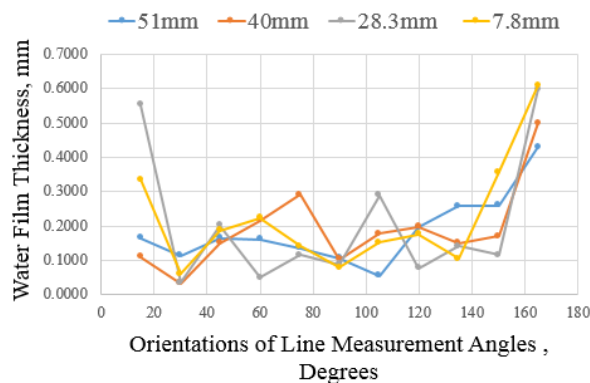


Figure-18. Graph of water film thickness for three different pitch tubes.

The comparative graph of Figure-18 shows that water film thickness is high at 15 and 165 degrees. It is approximated a point in which water film falls from stabilizer tube above it where water film falls at angle of 0 degree. The angle of 0 degree is the point where water falling film collides with test tube. Water molecules will be displaced out of the point with high velocities. As a result, some yellow contour existed along this point. The thickness of water film at this angle is unable to be measured. This local space is completely filled by falling water from upper tube. The film thickness is reduced when approach at orientation angle of 90°. It is then increased gradually as it passed through this angle. Water molecules with inherent properties were also accumulated at the bottom of the upper tube.

Table-5. Data Comparison with Equation 1.

The CFD results of film thickness at orientation angle of 90°				Result of equation 1 (mm)
Pitch tubes (mm)				
70.05	59.05	47.35	26.85	
0.1065	0.1020	0.0863	0.0785	0.22

Table-6. Data comparison with equation 2 for 59.05mm pitch tube.

Angle (°)	Film thickness (mm)	
	Equation 2	CFD results
15	1.2066	0.1102
30	0.9688	0.0325
45	0.8631	0.1491
60	0.8067	0.2152
75	0.7779	0.2904
90	0.7689	0.1020
105	0.6786	0.1777
120	0.7038	0.1969
135	0.7530	0.1505
150	0.8452	0.1695
165	1.0527	0.5000

CONCLUSIONS

Based on the simulation results, the thickness of sheet mode varies with orientation angles. These characteristics are affected by many factors, such as pitch tube, tube diameter and pressures. The different setting of parameters in Ansys Fluent such mesh size also lead to slightly different results. The existing literature has been reviewed extensively. The current numerical results are so far in agreement with the results from the literatures. The pitch tube of 70.05mm is a CFD model produced the thinnest film. The numerical tool chosen for the present study, Fluent, has enabled close examination of the flow field. Further work is in progress with the addition of experimental data.

REFERENCES

- [1] M. I. Mohamed. 2007. Flow behavior of liquid falling film on a horizontal rotating tube. *Exp. Therm. Fluid Sci.* 31(4): 325–332.
- [2] R. Armbruster and J. Mitrovic. 1998. Evaporative cooling of a falling water film on horizontal tubes. *Experimental Thermal and Fluid Science.* 18(3): 183–194.
- [3] J. Chen, R. Zhang, and R. Niu. 2015. Numerical simulation of horizontal tube bundle falling film flow pattern transformation. *Renewable Energy.* 73: 62–68.
- [4] V. Subramaniam and S. Garimella. 2014. Numerical study of heat and mass transfer in lithium bromide-water falling films and droplets. *International Journal of Refrigeration.* 40: 211–226.



- [5] L. Luo, G. Zhang, J. Pan and M. Tian. 2013. Flow and heat transfer characteristics of falling water film on horizontal circular and non-circular cylinders. *Journal of Hydrodynamics, Ser. B.* 25(3): 404-414.
- [6] B. Ruan, A. M. Jacobi and L. Li. 2009. Effects of a counter current gas flow on falling-film mode transitions between horizontal tubes. *Experimental Thermal and Fluid Science.* 33(8): 1216-1225.
- [7] G. Ribatski and A. M. Jacobi. 2005. Falling-film evaporation on horizontal tubes-a critical review. *International Journal of Refrigeration.* 28(5): 635-653.
- [8] F. Jafar, G. Thorpe and O. F. Turan. 2007. Liquid film falling on horizontal circular cylinders. 16th Australasian Fluid Mechanics Conference (AFMC). 1193-1200.
- [9] A. M. Abed, M. A. Alghoul, M. H. Yazdi, A. N. Al-Shamani and K. Sopian. 2014. The role of enhancement techniques on heat and mass transfer characteristics of shell and tube spray evaporator: a detailed review. *Applied Thermal Engineering.* 75: 923-940.
- [10] H. Hou, Q. Bi, H. Ma and G. Wu. 2012. Distribution characteristics of falling film thickness around a horizontal tube. *Desalination.* 285: 393-398.
- [11] F. A. Jafar, G. R. Thorpe and O. F. Turan. 2009. Flow mode characterisation of liquid films falling on horizontal plain cylinders. In *Proceedings of the 7th International Conference on CFD in the Minerals and Process Industries.* 1-6.
- [12] A. Cipollina, G. Micale and L. Rizzuti (Eds.). 2009. *Seawater desalination: conventional and renewable energy processes.* Springer Science & Business Media.